BeBeC-2014-02

SOUND SOURCE LOCALIZATION VIA ELASTIC NET REGULARIZATION

Xiaodong Li, Weiming Tong and Min Jiang
School of Energy and Power engineering, Beihang University
100191, Beijing, China

ABSTRACT

Most phased microphone array algorithms solve liner equations to localize sound sources. Since only a small portion of the source scanning region is expected to possess strong sources, the solutions of these equations would be sparse. In this paper, the elastic net regularization technique is proposed to solve the linear equations for sound source localization. Numerical validation results show that the elastic net regularization technique could improve both the resolution and accuracy compared with DAS (Delay-and-Sum) beamforming and DAMAS (Deconvolution Approach for the Mapping of Acoustic Sources) algorithm, particularly for cases under low signal-to-noise ratios. To demonstrate the advantage of the elastic net regularization, the NACA0012 airfoil self-noise sources are localized based on a direct numerical simulation database. Results also show that methods based on elastic net regularization have better performance than DAS beamforming and DAMAS algorithm.

1 INTRODUCTION

Phased microphone array technique has been widely used in aeroacoustic investigations. In the last decades, a number of sound source localization methods have been developed, including near-field acoustic holography [14], beamforming [12], acoustic inverse methods [6, 10, 11] and so on. The most commonly used beamforming algorithm in practice is DAS beamforming. DAS beamforming is very robust, but it suffers from high sidelobe and low resolution [7]. Therefore, many advanced methods are developed to improve its performance, such as DAMAS algorithm [2] and CLEAN-SC (CLEAN based on spatial source coherence) [13]. Later, DAMAS2 and DAMAS3 algorithm are proposed to simplify DAMAS algorithm to reduce CPU time [4]. A linear programming method is also used to solve the linear equations established by DAMAS algorithm to improve the computation efficiency [5].

Most beamforming methods cannot ensure good results when signal-to-noise ratio (SNR) is rather low [15]. In order to improve its performance in low SNR, convex optimization methods based on L1 norm constraints are applied nowadays [1, 15]. Yardibi [15] established SC-DAMAS algorithm based on L1 norm constraints and Bai [1] used L1 norm constraints to design array shape. Since sound source localization is a fundamentally inverse problem and L2 norm regularization is widely used to solve discrete inverse problems [10, 11]. To combine the good characteristic of L1 norm and L2 norm, mixed elastic net regularization methods are proposed by Zhou [16] to solve regression problems.

The primary objective of the current work is to investigate the feasibility of using elastic net regularization methods in the sound source localization problems. Linear equations established by DAMAS algorithm and CSM (cross spectrum matrix) are both solved by elastic net regularization method. After validation, this source localization methods based on elastic net regularization are used to localize NACA0012 airfoil self-noise sources. Time-dependent pressure data for phased array calculations are provided by numerical simulation using highly accurate Computational Aeroacoustics (CAA) approach.

The rest of the paper is organized as follows. Section 2 provides an introduction to elastic net regularization. This is followed by a brief description of beamforming methods, including DAS beamforming, DAMAS algorithm and methods based on elastic net regularization. The numerical validations of the proposed source localization methods based on elastic net regularization are given in Section 3. In Section 4, this method is applied to the localization of airfoil self-noise sources based on numerical simulation database. The concluding remarks are given in section 5.

2 INTRODUCTION TO ELASTIC NET REGULARIZATION

Most of the phased microphone array algorithms establish linear equations which can be written as

$$\boldsymbol{Ax} = \boldsymbol{b}, \boldsymbol{A} \in \mathbb{C}^{M\times N}, \boldsymbol{x} \in \mathbb{C}^{N}, \boldsymbol{b} \in \mathbb{C}^{M} \tag{1}$$

These linear equations are based on inverse problem and usually ill-conditioned. Therefore, solving these equations directly by single value decomposition probably lead to wrong results because $\boldsymbol{A}$ or $\boldsymbol{b}$ can be contaminated by noise. L2 norm based Tikhonov regularization is proposed to solve these ill-conditioned equations[3, 10, 11]

$$\min_{\boldsymbol{x}}\{\|\boldsymbol{Ax}-\boldsymbol{b}\|_2^2 + \lambda\|\boldsymbol{x}\|_2^2\} \tag{2}$$

where λ is the regularization parameter which can be determined by generalized cross function (GCV) or L-curve method. The solutions of L2 norm regularization typically have non-zero values associated with all $\boldsymbol{x}$. To obtain sparse solution, L1 norm regularization is often applied

$$\min_{\boldsymbol{x}}\{\|\boldsymbol{Ax}-\boldsymbol{b}\|_2^2 + \lambda\|\boldsymbol{x}\|_1\} \tag{3}$$

To combine the advantages of L1 and L2 norm, an elastic net regularization is employed in this paper for the solutions that have many zero elements and the non-zero elements are compact. The elastic net regularization can be expressed as

$$\min_{\boldsymbol{x}}\{\|\boldsymbol{Ax}-\boldsymbol{b}\|_2^2+\lambda_1\|\boldsymbol{x}\|_1+\lambda_2\|\boldsymbol{x}\|_2^2\} \tag{4}$$

The objective function of elastic net regularization is convex and can be solved efficiently by Matlab toolbox CVX. CVX uses interior point method to solve convex optimization problems. To validate the elastic net regularization technique, linear equations created by Hilbert matrix are solved by the proposed regularization method. The matrix $\boldsymbol{A}$ has the dimension of 100×100, and the condition number of $\boldsymbol{A}$ is 9.6×10^{19}, which means the system is ill-conditioned. The true value of $\boldsymbol{x}$ satisfies: $x(51\sim61)=10$, and the others are zero. L2 norm regularization, L1 norm regularization and elastic net regularization are all applied in this validation case. The results shown in Fig. 1 indicate that elastic net regularization yield the best results for this case. The L2 norm regularization keeps all the solutions non-zero and does not encourage sparsity. The results of L1 norm regularization cannot show the characteristic of continuous distribution. Further test shows that when matrix $\boldsymbol{A}$ or $\boldsymbol{b}$ is contaminated by noise, elastic net regularization could give better result.

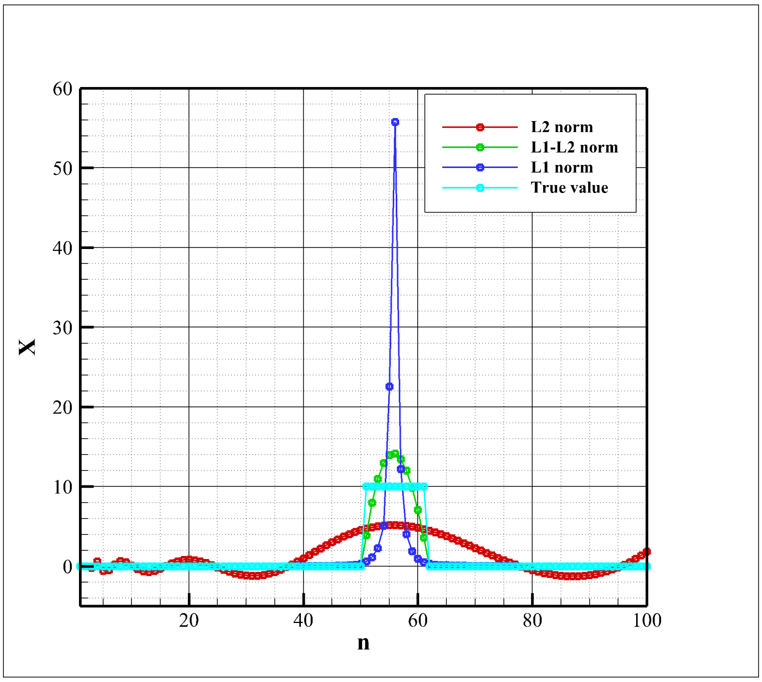

Figure 1: Results of regularization calculation

3 SOURCE LOCALIZATION METHODS

3.1 Methods based on elastic net regularization

The microphone number of the phased array system is assumed to be M. The sound source scanning region consists of N grid points and each grid point is supposed to be a monopole point source. The sound pressure in frequency domain received by the microphones then can be expressed as

$$\boldsymbol{p} = \boldsymbol{A}\boldsymbol{s} + \boldsymbol{e}, \boldsymbol{p} \in \mathbb{C}^M, \boldsymbol{A} \in \mathbb{C}^{M\times N}, \boldsymbol{s} \in \mathbb{C}^N, \boldsymbol{e} \in \mathbb{C}^M \tag{5}$$

where $\boldsymbol{A} = (\boldsymbol{a}_1, \ldots, \boldsymbol{a}_N)$, $\boldsymbol{a}_n = (e^{-jkr_{n,1}}/r_{n,1}, \ldots, e^{-jkr_{n,M}}/r_{n,M})^T$ is the array response vector, and $r_{m,n}$ is the distance from the n^{th} sound source scanning grid to the m^{th} array microphone. k is the wave number, $\boldsymbol{s}$ is the source waveform, and $\boldsymbol{e}$ represents the contamination noise. Suppose that the contamination noise is uncorrelated with the sound sources, the cross spectrum matrix (CSM) is defined by

$$\boldsymbol{G} = \langle \boldsymbol{p}\boldsymbol{p}^H \rangle = \boldsymbol{A}\langle \boldsymbol{s}\boldsymbol{s}^H \rangle \boldsymbol{A}^H + \langle \boldsymbol{e}\boldsymbol{e}^H \rangle \tag{6}$$

where $(\cdot)^H$ denotes the conjugate transpose and $\langle\cdot\rangle$ denotes the average value. When the sound sources are supposed to be uncorrelated with each other, $\langle \boldsymbol{s}\boldsymbol{s}^H \rangle = diag(q_1, \ldots, q_n, \ldots, q_N)$, and $q_n = \langle s_n {s_n}^* \rangle$ is the source power of the n^{th} grid. (6) can be rewritten as linear equations

$$\boldsymbol{R} = \boldsymbol{H}\boldsymbol{Q} + \boldsymbol{E}, \boldsymbol{R} \in \mathbb{C}^{M^2}, \boldsymbol{H} \in \mathbb{C}^{M^2\times N}, \boldsymbol{Q} \in \mathbb{R}^N, \boldsymbol{E} \in \mathbb{C}^{M^2} \tag{7}$$

where

$$R_{(i-1)\times M+j} = G_{i,j}, H_{(i-1)\times M+j,n} = A_{i,n} \times {A_{j,n}}^*, Q_n = q_n, E_{(i-1)\times M+j} = \langle e_i \times {e_j}^* \rangle$$

$$i, j = 1, \ldots, M, n = 1, \ldots, N$$

where $(\cdot)^*$ denotes the complex conjugate of the argument. When the contamination noise is white Gaussian noise, of which the mean value is zero and variance is σ^2 and all are uncorrelated, then $\langle \boldsymbol{e}\boldsymbol{e}^H \rangle = \sigma^2 \boldsymbol{I}$. When the sound sources are correlated, the source covariance matrix $\langle \boldsymbol{s}\boldsymbol{s}^H \rangle$ is not a diagonal matrix, whose off-diagonal element denotes the correlation between different sources. At this time Eq. (6) can be rewritten as linear equations

$$\boldsymbol{R} = \boldsymbol{H}\boldsymbol{Q} + \boldsymbol{E}, \boldsymbol{R} \in \mathbb{C}^{M^2}, \boldsymbol{H} \in \mathbb{C}^{M^2\times N^2}, \boldsymbol{Q} \in \mathbb{C}^{N^2}, \boldsymbol{E} \in \mathbb{C}^{M^2} \tag{8}$$

where

$$R_{(i-1)\times M+j} = G_{i,j}, H_{(i-1)\times M+j,(k-1)\times N+l} = A_{i,k} \times {A_{j,l}}^*, Q_{(k-1)\times N+l} = \langle s_k {s_l}^* \rangle$$

$$E_{(i-1)\times M+j} = \langle e_i \times e_j^* \rangle, i, j = 1, \ldots, M, k, l = 1, \ldots, N$$

The number of unknown variables of Eq. (8) is much larger than that of Eq. (7).

DAS beamforming estimates the source power of the n^{th} grid by

$$b_n = \frac{1}{M^2} {\boldsymbol{w}_n}^H \boldsymbol{G} \boldsymbol{w}_n \tag{9}$$

where $\boldsymbol{w}_n$ represents the steering vector which is defined by

$$\boldsymbol{w}_n = \frac{1}{r_{n,o}} [r_{n,1} e^{-jkr_{n,1}}, \ldots, r_{n,m} e^{-jkr_{n,m}}, \ldots, r_{n,M} e^{-jkr_{n,M}}]^T \tag{10}$$

where $r_{n,o}$ denotes the distance from the n^{th} grid to the array center. DAMAS algorithm assumes that the sources are independent and constructs a linear system of equations that relate the DAS results to the source power of every scanning grid. The linear equations are

$$\begin{pmatrix} b_1 \\ \cdots \\ b_N \end{pmatrix} = \frac{1}{M^2} \begin{pmatrix} |\boldsymbol{w}_1{}^H \boldsymbol{a}_1|^2 & \cdots & |\boldsymbol{w}_1{}^H \boldsymbol{a}_N|^2 \\ \cdots & \cdots & \cdots \\ |\boldsymbol{w}_N{}^H \boldsymbol{a}_1|^2 & \cdots & |\boldsymbol{w}_N{}^H \boldsymbol{a}_N|^2 \end{pmatrix} \begin{pmatrix} q_1 \\ \cdots \\ q_N \end{pmatrix} \tag{11}$$

If uniform flow exists in the x direction, the array response and steering vector should be changed to

$$a_{n,m} = \frac{1}{(rD)_{n,m}} e^{-jk[(rD)_{n,m} - M_0(x_m - \tilde{x}_n)]/\beta^2}, w_{n,m} = \frac{(rD)_{n,m}}{(rD)_{n,o}} e^{-jk[(rD)_{n,m} - M_0(x_m - \tilde{x}_n)]/\beta^2} \tag{12}$$

where $(rD)_{n,m} = \sqrt{(\beta r_{n,m})^2 + [M_0(x_m - \tilde{x}_n)]^2}, \beta = \sqrt{1 - M_0{}^2}$, x_m is the x-coordinate of m^{th} microphone and $\tilde{x}_n$ is the x-coordinate of n^{th} scanning grid.

In general, only a small portion of the source scanning region is expected to possess strong sources. Therefore, the solution of Eq. (7) and (11) should be sparse. At the same time, the sources may be isolated point sources or distributed sources and contamination noise can be strong. L1 norm and L2 norm based elastic net regularization can be a good alternative for this problem. Furthermore, Matlab toolbox CVX is a useful tool for solving the linear equations established by elastic net regularization. The unknown variables in Eq. (7) and (11) are real which represent the sound source power and should be non-negative. The methodology of the phased microphone array algorithm is illustrated in Fig. 2.

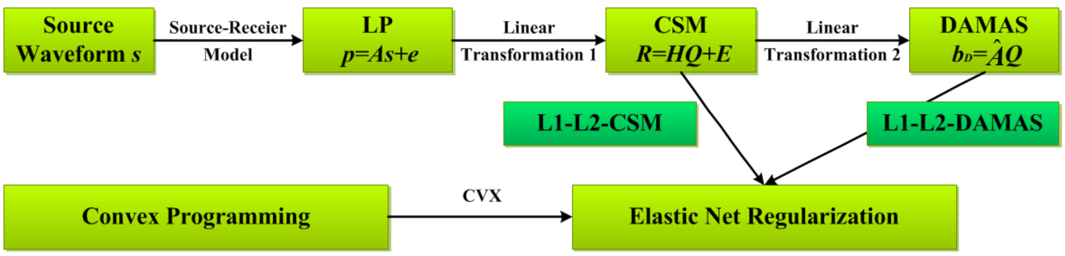

Figure 2: Methodology of phased microphone array algorithms

The regularization parameters are very important to the solutions. However, this parameter is unknown and usually chosen empirically. Since the number of main eigenvalues of the CSM represents the number of uncorrelated sources, λ_1 is chosen according to number of main eigenvalues of CSM and the SNR (signal-to-noise ratio). Numerical tests show that a good choice for λ_2 is closed equal to $(0.1 \sim 0.5)\lambda_1$. For simplicity, solving Eq. (7) by elastic net regularization is called L1-L2-CSM, and solving Eq. (11) by elastic net regularization is called L1-L2-DAMAS.

3.2 Numerical results

In this section, two test cases are presented to validate the feasibility of the proposed sound source localization methods based on elastic net regularization. Both isolated point sources and distributed line source are considered. Furthermore, the validation is also performed under rather low SNR.

In this section, array shape is the Large Aperture Directional Array (LADA) [7] which consists 35 microphones. Distance between the source scanning region and the phased array is 1.0m. The source scanning region is 1.0m×1.0m, and the scanning grids number is 41×41=1681, uniform spacing. Sampling frequency is 65536Hz and sampling time is 10s. The frequency domain pressure signals are calculated by Fast Fourier Transform (FFT). FFT is done with 4096 points and Hanning window is added, of which overlapping ratio is 50 percent.

Firstly, a single frequency point source is simulated with the source power as 10 and frequency as 3200Hz. Time domain signals are simulated without noise. Results of DAS beamforming, DAMAS algorithm, L1-L2-DAMAS and L1-L2-CSM are shown in Fig. 3. It is clear that DAS beamforming suffers from low resolution and the source location and power are calculated accurately by the other three methods.

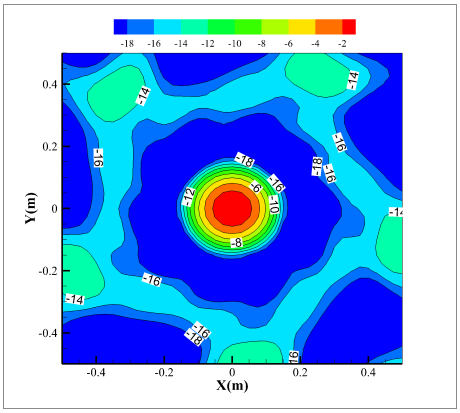

(a) DAS

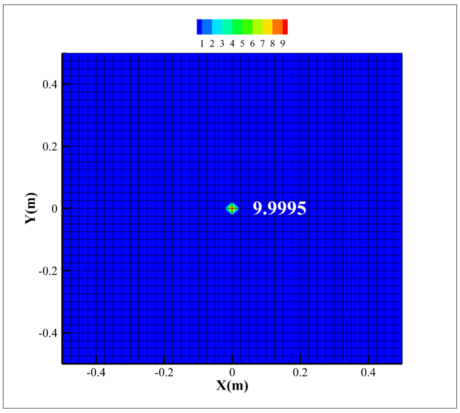

(b) DAMAS

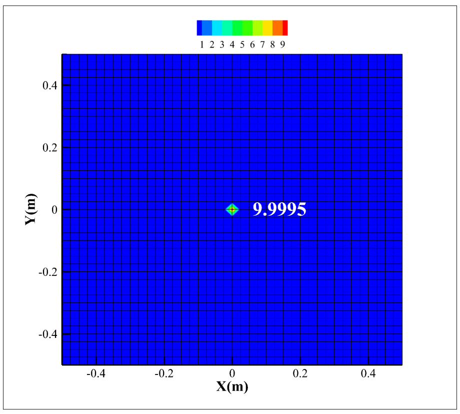

(c) L1-L2-DAMAS

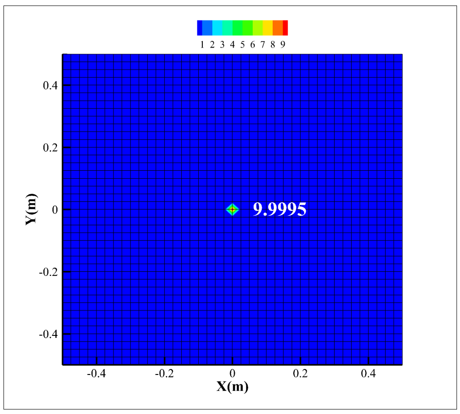

(d) L1-L2-CSM

Figure 3: Results of source localization without noise (one source)

Secondly, four uncorrelated broadband point sources and uncorrelated line source are simulated with Gaussian-distributed random numbers. The line source consists of 35 uncorrelated point sources. The location of the four uncorrelated point sources is (0,0)m, (0.2,0.2)m, (-0.2,0.2)m and (0.2,-0.2)m. The power of the four sources is 0.1197, 0.1217, 0.1188, and 0.1203 respectively. The length of the line source is 0.4m, from -0.2m to 0.2m in the x-axis and the power of the line source is 4.2469. Time domain signals are simulated without noise and other conditions are the same as previous cases. Since no contamination noise is added, diagonal removal (DR) technique is not used in this case. Results of DAS beamforming, DAMAS algorithm, L1-L2-DAMAS and L1-L2-CSM are shown in Fig. 4 and Fig. 5. The red circle denotes the location of the real sound sources. It can be noticed that the sound sources are localized accurately. In the line source case, the relative error of source power is slightly larger than the other cases. This might be due to the fact that many sources are not on the source scanning grid points. This validation case indicates that DAMAS, L1-L2-DAMAS and L1-L2-CSM can be used to localize isolated point sources and distributed sources as well.

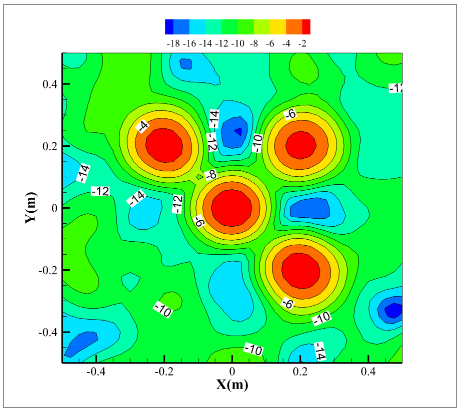

(a) DAS

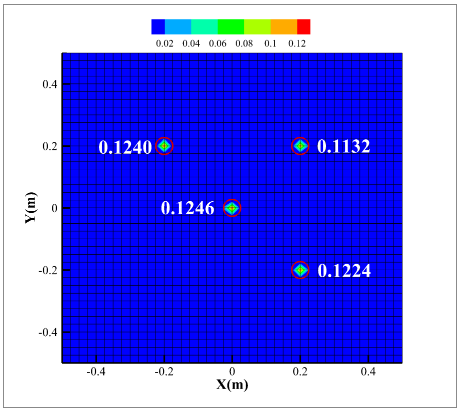

(b) DAMAS

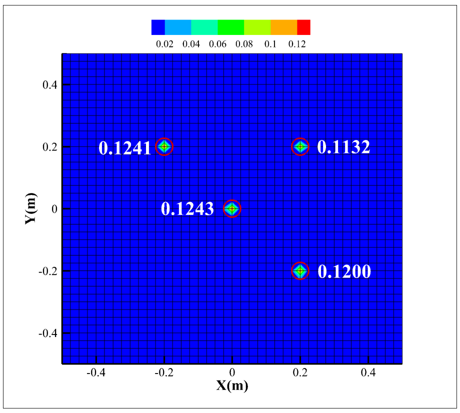

(c) L1-L2-DAMAS

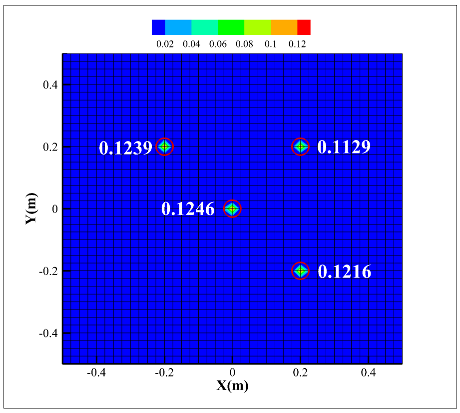

(d) L1-L2-CSM

Figure 4: Results of source localization without noise (four sources)

The Calculation times of three algorithms are listed in Table 1. DAMAS algorithm iterates 10000 steps in the current case. Obviously that methods based on elastic net regularization is

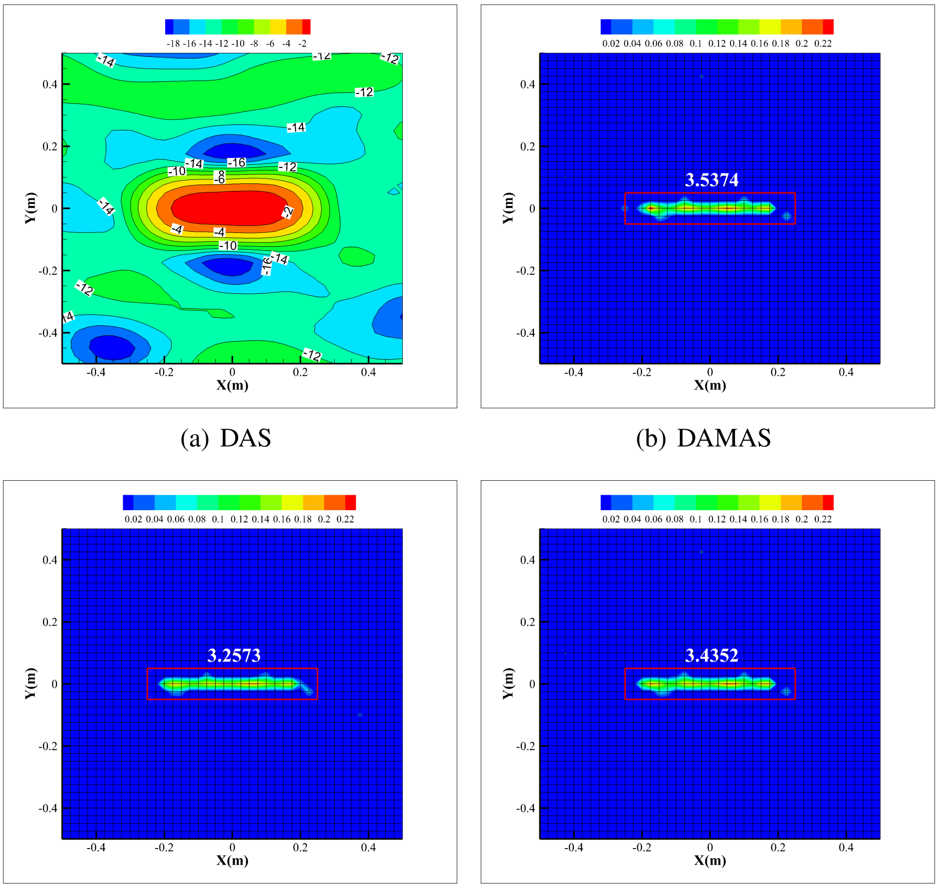

(a) DAS (b) DAMAS

(c) L1-L2-DAMAS (d) L1-L2-CSM

Figure 5: Results of source localization without noise (line source)

slightly slower than DAMAS algorithm. This is because our code is written in Fortran language and it needs to call external functions of Matlab to solve the elastic net regularization equations, which requires extra CPU time.

Table 1: Calculation time

Calculation times(s)	DAMAS	L1-L2-DAMAS	L1-L2-CSM
Four sources	856	936	1196
Line source	603	1024	1079

Finally, methods based on elastic net regularization are tested with rather low SNR. White Gaussian noise is added to the simulated time domain signals. The SNR is defined by

$$SNR = 10lg \frac{\frac{1}{M}\sum_{m=1}^{M} E\{{p_m}^2\}}{{\sigma_n}^2} \tag{13}$$

where $E\{p_m{}^2\}$ means the average power received by the m^{th} microphone and $\sigma_n{}^2$ is the variance of the noise, also is the noise's average power. Time domain signals are simulated with $SNR = -10dB$ for the four uncorrelated sources and line source respectively. Diagonal removal (DR) of CSM technique is used. DAS beamforming, DAMAS algorithm, L1-L2-DAMAS and L1-L2-CSM are all used to localize these sources. Results are shown in Fig. 6 and Fig. 7. The locations of real sources are marked by a red circle. The results show that DAS beamforming is very robust but with low resolution and high sidelobe. DAMAS algorithm would generate some pseudo sources. L1-L2-DAMAS and L1-L2-CSM lead to better results and the only disadvantage is that the sound power of the identified sources is smaller than the true value.

The comparison of Fig. 4, Fig. 5, Fig. 6 and Fig. 7 show that L1-L2-DAMAS and L1-L2-CSM can not only localize isolate point sources, but can also localize distributed sources. Furthermore, these two methods are more robust than DAMAS algorithm when the SNR is rather low.

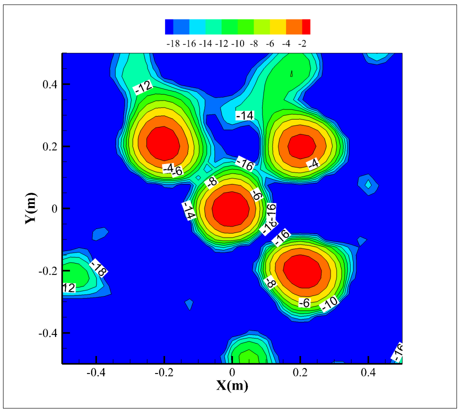

(a) DAS

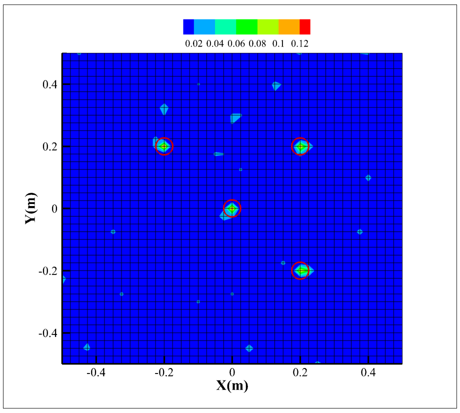

(b) DAMAS

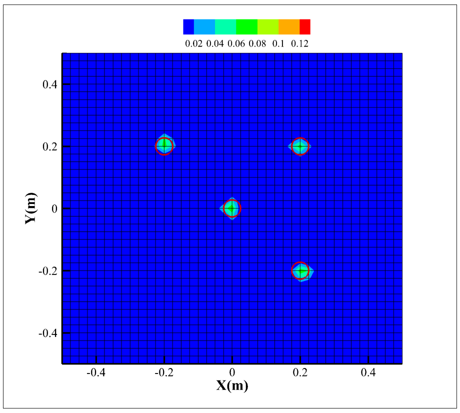

(c) L1-L2-DAMAS

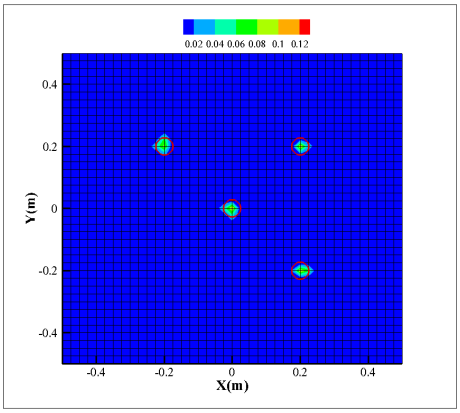

(d) L1-L2-CSM

Figure 6: Results of source localization with SNR=$-10dB$ (four sources)

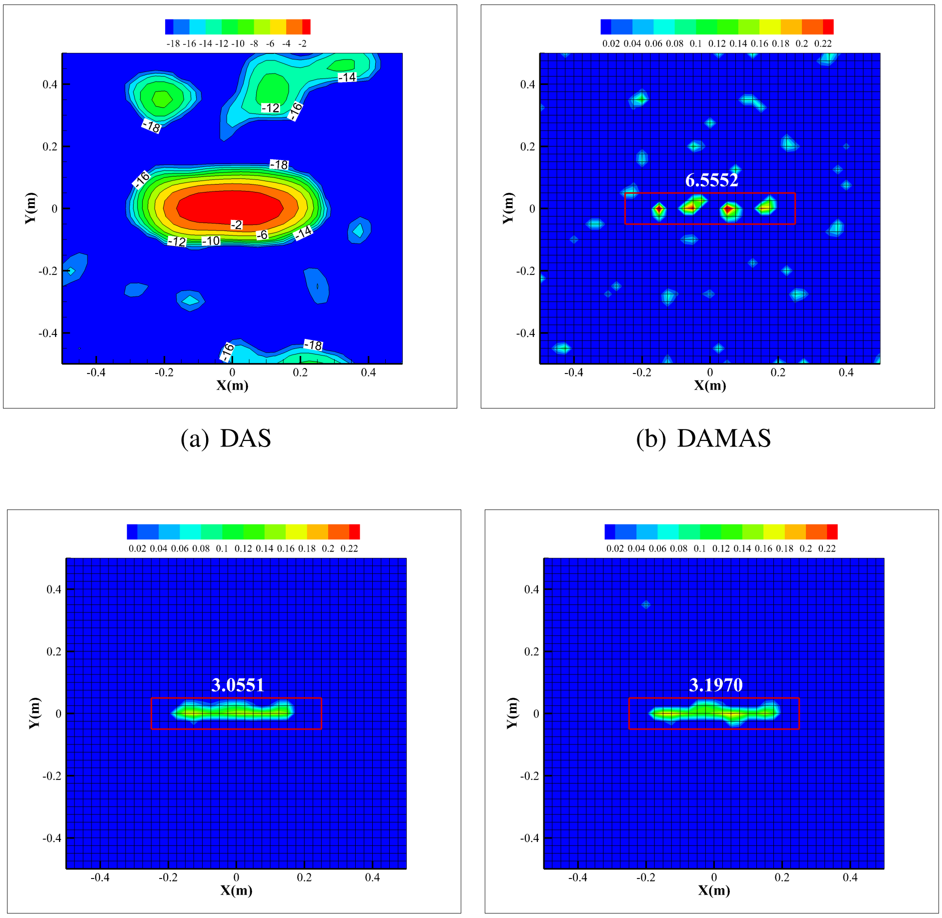

(a) DAS (b) DAMAS

(c) L1-L2-DAMAS (d) L1-L2-CSM

Figure 7: Results of source localization with SNR=$-10dB$ (line source)

4 LOCALIZATION OF NACA0012 AIRFOIL SELF-NOISE SOURCES

In this section, L1-L2-DAMAS and L1-L2-CSM are used to localize NACA0012 airfoil self-noise sources based on numerical data. Results are compared with those by DAS beamforming and DAMAS algorithm to demonstrate the advantage of elastic net regularization.

In the numerical simulation, the chord length of the airfoil is 0.1m and the angle of attack is zero degree. The Reynolds number is 4×10^5 and the Mach number is 0.17. More details of the numerical simulation can be referred to [9].

Figure 8 shows the configuration of the virtual phased microphone array in the current work. The NACA0012 airfoil is placed with its leading edge at the origin of the coordinate system. Five chords above the airfoil camber line places a phased microphone array. This array system is composed of virtual microphones that distributed in a straight line from -0.2m to 0.5m. Along the airfoil camber line from -0.1m to 0.4m, a scanning system that consists of 501 grid points is configured. Each grid point is considered as a potential monopole source in the phased array calculations. The region covered by the scanning grid is supposed as the dominant region responsible for the airfoil self-noise generation.

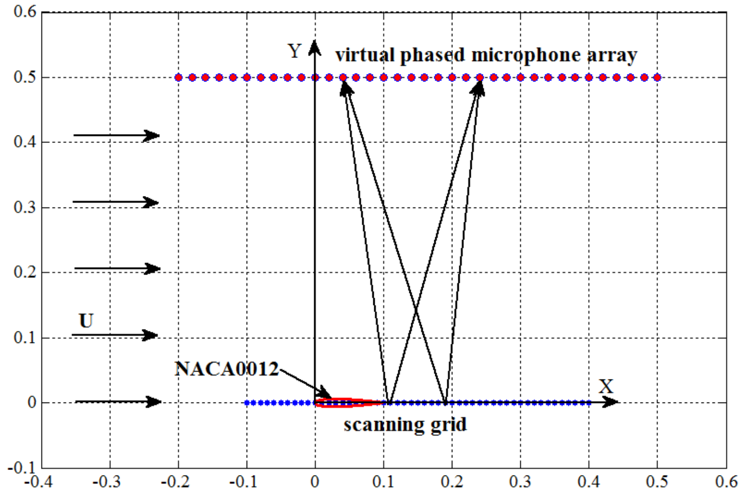

Figure 8: Sketch of the beamforming model

DAS beamforming, DAMAS algorithm, L1-L2-DAMAS and L1-L2-CSM are all used to localize the NACA0012 airfoil self-noise sources. All the identified source power are normalized by the maximum value and then displayed in dB. The x-coordinate denotes the streamwise location of the noise sources. The y-coordinate represents the frequency of identified noise sources. The two red solid lines marked by LE and TE denote the location of the airfoil leading and trailing edge respectively. Source localization results are shown in Fig. 9. The main sound source region is marked by a dashed box. From the results, it is clearly shown that the noise sources are mainly focused at about 3.4 kHz and the main sources region is located at the trailing edge. However, DAS beamforming results indicate that there are some sources located at the leading edge and far from the trailing edge, which is not consistent with many experimental results [8]. At the same time, the resolution is very low for DAS beamforming. When DAMAS algorithm is applied, resolution is improved, but the pseudo sources still exist. Regarding the results of L1-L2-DAMAS and L1-L2-CSM, the resolution is found to be improved. Furthermore, the power of the pseudo source at the leading edge is significantly reduced and other pseudo sources disappeared.

5 CONCLUSIONS

Elastic net regularization is applied to the phased microphone array technique. Linear equations established by DAMAS algorithm and CSM are both solved by elastic net regularization. The numerical validation is conducted both by the isolated uncorrelated point sources and uncorrelated line source cases. The two tests both show that methods based on elastic net regularization can not only improve the resolution and suppress sidelobe, but also obtain better results than DAMAS algorithm when the SNR is rather low. Furthermore, the advantage of elastic net regularization is demonstrated by the example of NACA0012 airfoil self-noise localization problem. Results of DAS beamforming, DAMAS algorithm and methods based on elastic net regularization all show that the dominant sources are at approximately 3.4 kHz, and mainly located at the airfoil trailing edge. However, the elastic net regularization can ensure more convincing results.

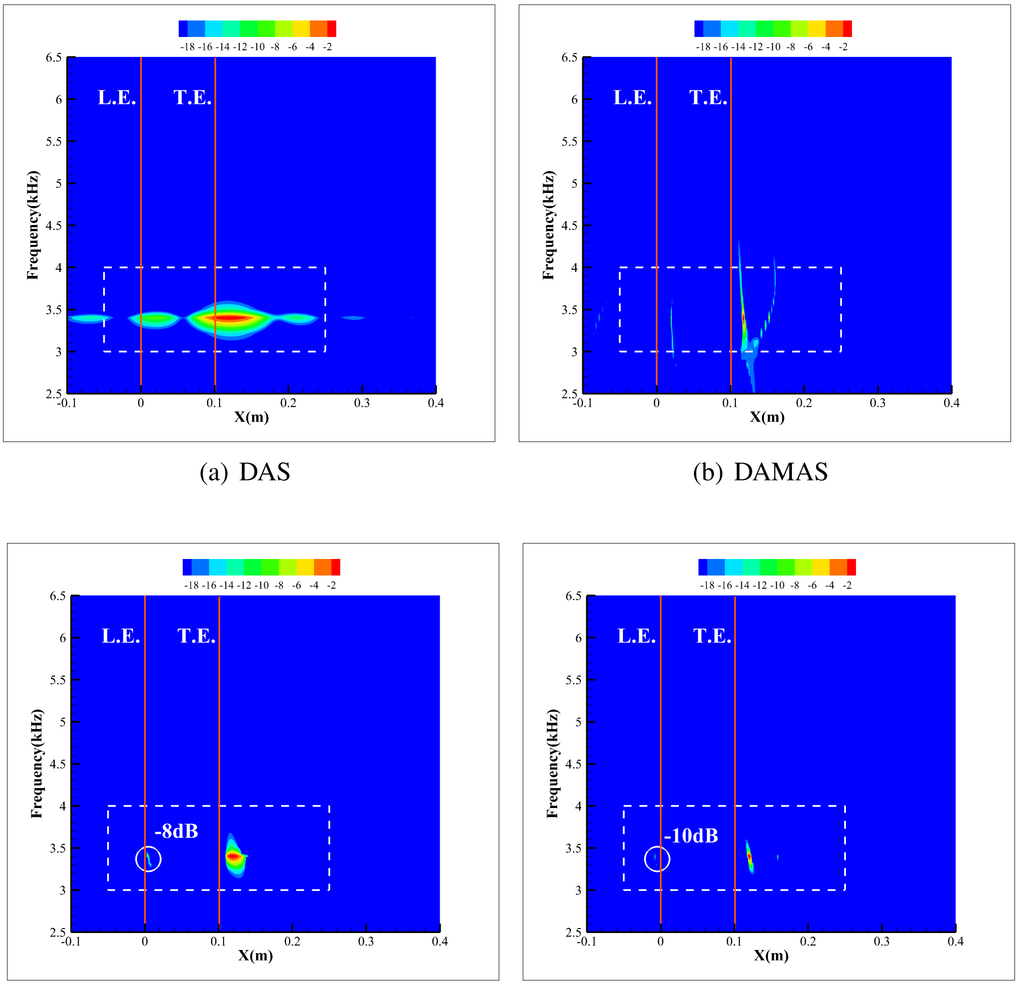

(a) DAS (b) DAMAS

(c) L1-L2-DAMAS (d) L1-L2-CSM

Figure 9: Results of NACA0012 airfoil self-noise sources localization

6 ACKNOWLEDGEMENT

This work is supported by grants from 973 Program-2012CB720202. The authors also would like to acknowledge the partial support from the 111 Project B07009 of China.

REFERENCES

[1] M. R. Bai and C. C. Chen. “Application of convex optimization to acoustical array signal processing.” *J. Sound Vib.*, 332, 6596–6616, 2013. doi:10.1016/j.jsv.2013.07.029.

[2] T. F. Brooks and W. M. Humphreys. “A deconvolution approach for the mapping of acoustic sources (DAMAS) determined from phased microphone arrays.” AIAA-2004-2954, 2004. 10th AIAA/CEAS Aeroacoustics Conference, Manchester, UK, May 10-12, 2004.

[3] D. Calvetti, S. Morigi, , L. Reichel, and F. Sgallari. “Tikhonov regularization and the L-curve for large discrete ill-posed problems.” *J. Comput. Appl. Math.*, 123, 423–446, 2000. doi:10.1016/S0377-0427(00)00414-3.

[4] R. P. Dougherty. “Extensions of DAMAS and benefits and limitations of deconvolution in beamforming.” AIAA 2005-2961, 2005. 11th AIAA/CEAS Aeroacoustics Conference, Monterey, California, May 23-25, 2005.

[5] R. P. Dougherty, R. C. Ramachandran, and G. Raman. “Deconvolution of sources in aeroacoustic images from pahsed microphone array using linear programming.” AIAA 2013-2210, 2013. 19th AIAA/CEAS Aeroacoustics Conference, Berlin, Germany, May 27-29, 2013.

[6] K. R. Holland and P. A. Nelson. “The application of inverse methods to spatially-distributed acoustic sources.” *J. Sound Vib.*, 332, 5727–5747, 2013. doi:10.1016/j.jsv.2013.06.009.

[7] W. M. Humphreys, T. F. Brooks, W. M. Hunter, and K. R. Meadows. “Design and use of microphone directional arrays for aeroacoustic measurements.” AIAA-98-0471, 1998. 36th Aerospace Sciences Meeting & Exhibit, Reno, NV, January 12-15, 1998.

[8] F. V. Hutcheson and T. F. Brooks. “Effects of angle of attack and velocity on trailing edge noise determined using microphone array measurements.” *Int. J. Aeroacoustics*, 5, 39–66, 2006. doi:10.1260/147547206775220425.

[9] M. Jiang, X. D. Li, and W. M. Tong. “Identification and localization of airfoil noise sources at low angles of attack.” AIAA 2014-0018, 2014. 52th Aerospace Science Meeting, National Harbor, Maryland, January 13-17, 2014.

[10] X. D. Li and S. Zhou. “Spatial transformation of the discrete sound field from a propeller.” *AIAA J.*, 34, 1097–1102, 1996. doi:10.2514/3.13198.

[11] J. Luo and X. D. Li. “An inverse aeroacoustic problem on rotor wake/stator interaction.” *J. Sound Vib.*, 322, 219–229, 2002. doi:10.1006/j.jsv.2001.3671.

[12] T. J. E. Mueller. *Aeroacoustic measurements*. Springer, Germany, 2002.

[13] P. Sijtsma. “CLEAN based on spatial source coherence.” *Int. J. Aeroacoustics*, 6, 357–374, 2007. doi:10.1260/147547207783359459.

[14] E. G. Williams, J. D. Maynard, and E. Skudrzyk. “Sound source reconstructions using a microphone array.” *J. Acoust. Soc. Am.*, 68, 340–344, 1980. doi:10.1121/1.384602.

[15] T. Yardibi, J. Li, P. Stoica, and L. N. Cattafesta. “Sparsity constrained deconvolution approaches for acoustic source mapping.” *J. Acoust. Soc. Am.*, 123, 2631–2642, 2008. doi:10.1121/1.2896574.

[16] H. Zhou and T. Hastie. “Regularization and variable selection via the elastic net.” *J. R. Statist Soc. B*, 67, 301–320, 2005. doi:10.1111/j.1467-9868.2005.00503.x.